Electronic Supplementary Material (ESI) for ChemComm.

Supporting information

$[Fe^{III}(Tp)(CN)_3]^-$ Scorpionate Complex as a Building Block for designing Ion-Storage Host

Juan R. Jimenez *et al*.

Experimental section

General procedures

Reagents and solvents purchased from commercial sources were used as received. All the reactions were conducted in oven-dried glassware under aerobic conditions. $(NBu_4)[Fe(Tp)(CN)_3]$ was synthesized using the synthesis reported by Lescouëzec *et al.*[1] but using Bu_4NCl as counter ion.

Synthesis and characterizations of $\{Fe^{III}(Tp)(CN)_3\}_2\{Ni^{II}(H_2O)_2\}\cdot 4H_2O$ and $\{Fe^{III}(Tp)(CN)_3\}_2\{Ni^{II}(CH_3OH)_2\}\cdot CH_3OH\cdot 0.5H_2O$

To a solution of $Ni(NO_3)\cdot 6H_2O$ (0.5 mmol, 145 mg) in 100 mL of methanol/water (7/3) was added dropwise a solution of $(NBu_4)[Fe(Tp)(CN)_3]$ (1 mmol, 588 mg) in the same solvent mixture. The resulting solution was stirred for 12 h. A red-orange powder was obtained, which was filtered and dried in air at room temperature. Yield : 68%. Anal. Calcd for $C_{24}H_{32}B_2Fe_2N_{18}NiO_6$ C 33.49; H 3.74; N 29.29. Found C 33.38; H 3.60; N 29.07.
Crystals of **1** can be obtained *via* single-crystal to single-crystal transformation by drying in air over several days crystals of the parent methanolic compound $\{Fe^{III}(Tp)(CN)_3\}_2\{Ni^{II}(CH_3OH)_2\}\cdot CH_3OH\cdot 0.5H_2O$ (**1'**, prepared according to You et al.[2]).

We have compared the FTIR spectra of **1** in both crystal and powder phases in order to see whether or not there are any remarkable structural changes. The spectra (see Figure S3) exhibit intense cyanide stretching vibrations at 2164 cm^{-1} and 2167 cm^{-1} on the powder and crystal phases respectively, characteristic of bridging Fe^{III}-CN-Ni^{II}. Both phases show at 2124 cm^{-1} the stretching characteristic of the terminal Fe^{III}-CN cyanide ligand. No changes were observed on the absorption bands at 1492, 1424, 1409, 1386, 1294 and 902 cm^{-1} which are ascribed to the anionic Tp ligand as well as the broad absorption at 2541 cm^{-1} which is due to the ν(B-H) stretching vibration.

Physical measurements

Elemental analyses for C, H, and N were performed on a Perkin-Elmer 240C analyser. **FTIR spectroscopic data** were carried out on a Tensor Bruker instrument working in the ATR mode and collected in the 400-4000 cm-1 range at room temperature. **X-ray powder diffraction** patterns were collected on a Philips X'pert Pro diffractometer using Co-Kα1 monochromatic radiation (λ =1.78901 Å) and equipped with a X'celerator linear detector. The

[1] R. Lescouëzec, F. Lloret, M. Julve, J. Vaissermann, M. Verdaguer, *Inorg. Chem.* 2002, **41**, 5943.
[2] H.-R. Wen, C.-F. Wang, Y. Song, S. Gao, J.-L. Zuo, X. You, *Inorg. Chem.* 2006, **45**, 8942

thermogravimetric analysis (TGA) experiment was performed under air or N_2 flow up to 600 °C, with a heating rate of 5 K/min. The **X-ray absorption** spectra were measured in the transmission mode at room temperature at BL-9C of Photon Factory.

Magnetic measurements on $\{[Fe(Tp)(CN)_3]_2[Ni(H_2O)_2]\}\cdot 4H_2O$ were carried out with a SQUID magnetometer in the temperature range 1.9–300 K and under an applied field ranging from 250 to 2500 G. The magnetization measurements were done at 2.0 K in the range 0–7 T. The magnetic susceptibility data were corrected for the diamagnetic contribution of the constituent atoms through the Pascal constants and also for the sample holder.

Electrochemical measurements were conducted using the working electrodes which were prepared by mixing $\{[Fe(Tp)(CN)_3]_2[Ni(H_2O)_2]\}\cdot 4H_2O$, acetylene black, and polytetrafluoroethelene (100:30:10) into paste. CR2032-type coin cells were assembled inside an Ar-filled glove box (dew point < −100 °C) with a Li-metal counter electrode, a glass-fiber membrane separator and 1 M $LiClO_4$ in propylene carbonate electrolyte. The cyclic voltammetry was performed at the sweep rate of 0.2 mV/s between 2.0−4.0 V vs. Li/Li^+. The open-circuit potentials were recorded by repetition of alternating the galvanostatic charge or discharge at 10 mA/g for 12 min and relaxation for 20 minutes. Galvanostatic charge-discharge curves were measured at a specific current of 12 mA/g between 2.5−4.0 V (vs. Li/Li^+). **Ex situ XRD** patterns were measured on a RIGAKU Smart Lab diffractometer.

Single-crystal-XRD : Frames were collected on a Bruker Kappa APEXII diffractometer at room temperature. Data collection were performed with APEX2 suite (BRUKER). Unit-cell parameters refinement, integration and data reduction were carried out with SAINT program (BRUKER). SADABS (BRUKER) was used for scaling and multi-scan absorption corrections.

An orange single crystal of $\{Fe^{III}(Tp)(CN)_3\}_2\{Ni^{II}(CH_3OH)_2\}\cdot CH_3OH\cdot 0.5H_2O$ was mounted onto a glass fiber and placed on the diffractometer. The unit cell parameters found were those previously reported by You et *al*. Then the crystal was removed from the diffractometer and left in air for a few days. Despite an obvious degradation of the crystal quality, there is still diffraction signal after that period, allowing the determination of unit cell parameters fully coherent with the powder XRD measurements (see XRD patterns). A complete data collection was then carried out although the enlarged diffraction peaks and the low crystallographic resolution clearly limit the quality of the dataset.

In the WinGX suite of programs[3], the structure were solved with SHELXT-14[4] program and refined by full-matrix least-squares methods using SHELXL-14[5]. Non-metallic atoms were

[3] L. J. Farrugia, *Journal of Applied Crystallography* **1999**, *32*, 837–838.
[4] G. M. Sheldrick, *Acta Crystallographica Section A* **2015**, *71*, 3–8.

refined anisotropically while all others were refined isotropically due to the low number of data. Hydrogen atoms of the Tp ligand were placed at calculated positions. The Fourier difference maps do not show the presence of carbon atoms, indicating that MeOH molecules were replaced by water molecules in the crystal structure.

Crystal data for **1**. orange block-like crystals: $C_{24}H_{34}B_2Fe_2N_{18}NiO_7$, monoclinic, *C 2/c*, a = 28.851(7), b = 9.668(2), c = 13.718(3) Å, β = 101.205(11) °, V = 3753.4(16) $Å^3$, Z = 4, T = RT, μ= 5.233 mm^{-1}, 5013 reflections measured, 1250 independent (R_{int}= 0.0770), 780 observed [I≥2σ(I)], 118 parameters, final R indices R_1 [I≥2σ(I)] = 0.0800 and wR_2 (all data)= 0.248, GOF on F^2 = 1.03, max/min residual electron density = 0.69/-0.43 e.$Å^{-3}$.

[5] G. M. Sheldrick, *Acta Crystallographica Section C* **2015**, *71*, 3–8.

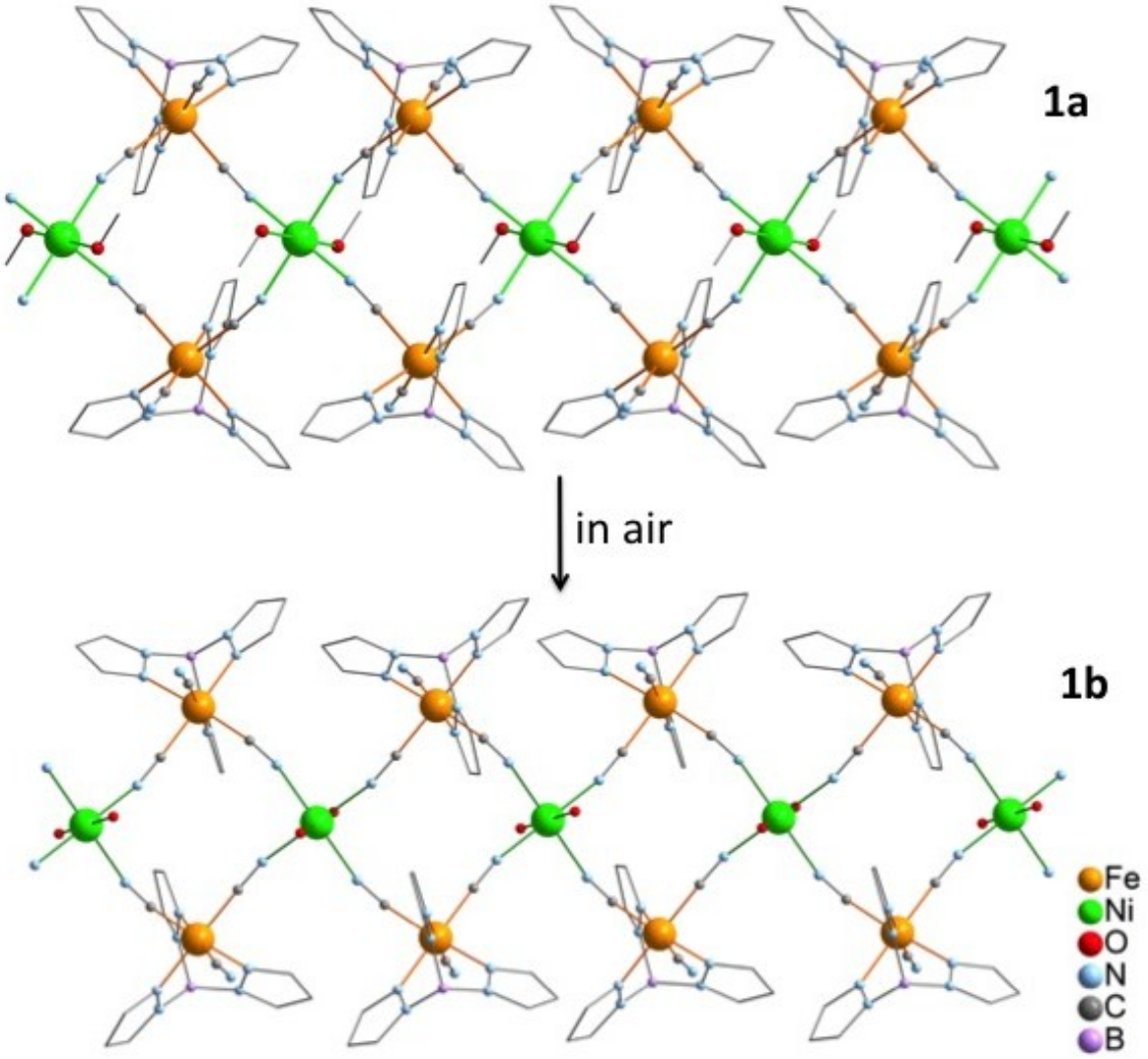

Figure S1. Single-crystal to single-crystal phase transition: perspective view of the crystal structure of $\{[Fe(Tp)(CN)_3]_2[Ni(H_2O)_2]\}\cdot 4H_2O$ (1b) obtained after leaving $\{[Fe(Tp)(CN)_3]_2[Ni(CH_3OH)_2]\}\cdot 1.0CH_3OH\ 0.5H_2O$ (1a) in air for 3 days.

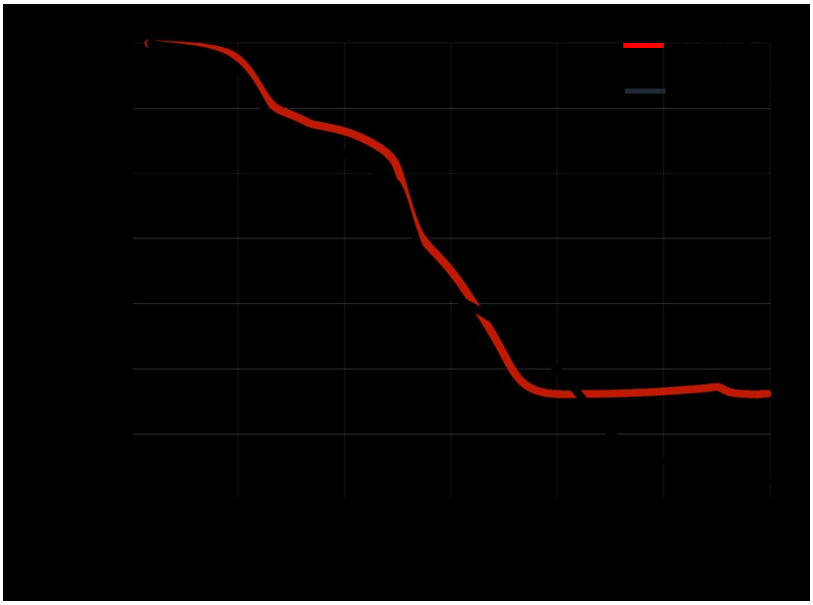

Figure S2. TGA of **1** at 2°C/min under N_2 and air flow in the temperature range 25-600°C.

The compound $\{[Fe(Tp)(CN)_3]_2[Ni(H_2O)_2]\}\cdot 4H_2O$ undergoes a weight loss between 90 and 100°C (*ca.* 10%), which corresponds to the removal of 4 H_2O lattice molecules. The material is stable under N_2 and air atmosphere up to ca. 260°C.

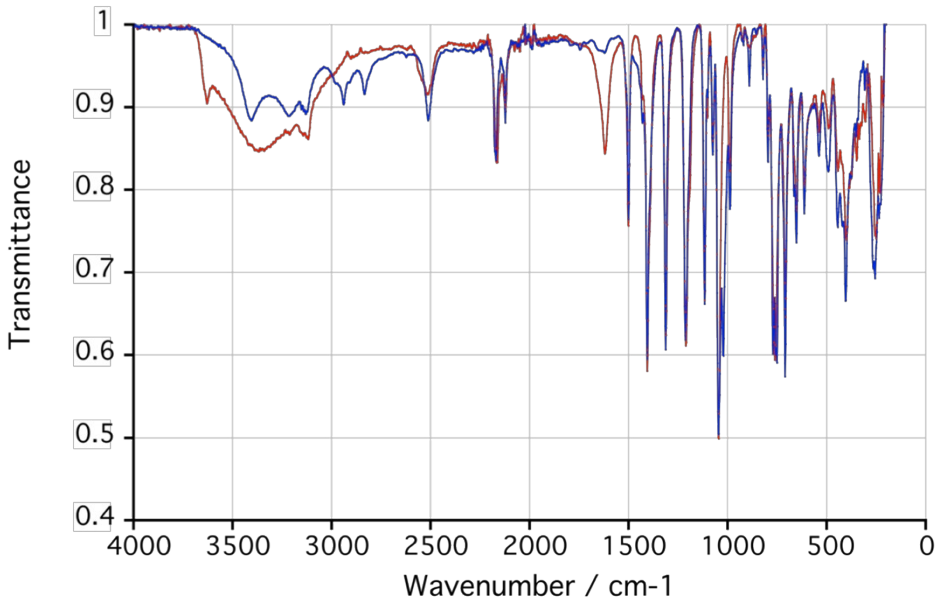

Figure S3. (Blue) FT-IR spectra of the single crystals of **1'** (blue) and of the compound **1** (red) which has been air dried for several days.

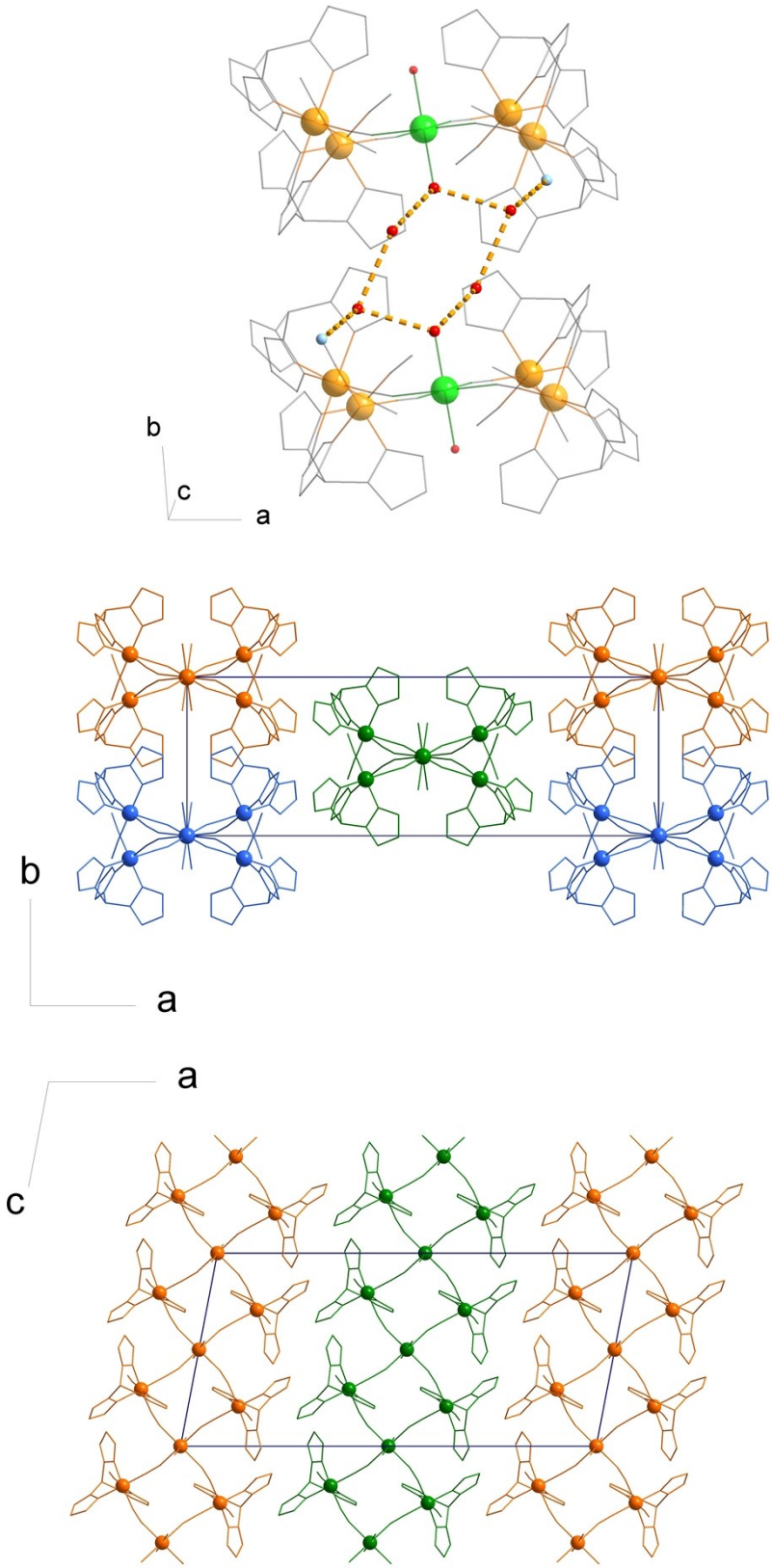

Figure S4. Intermolecular interactions in $\{[Fe(Tp)(CN)_3]_2[Ni(H_2O)_2]\}\cdot 4H_2O$. Top: view of the hydrogen-bond network between adjacent chains (doted lines are distances inferior to 3.1 Å);[6] Middle and bottom: view of the chains packing in the *ab* and *ac* planes.

[6] O···O distances: 2.812 (1); 2.967(1), 3.076(1) Å; O···N distance: 3.053(1) Å

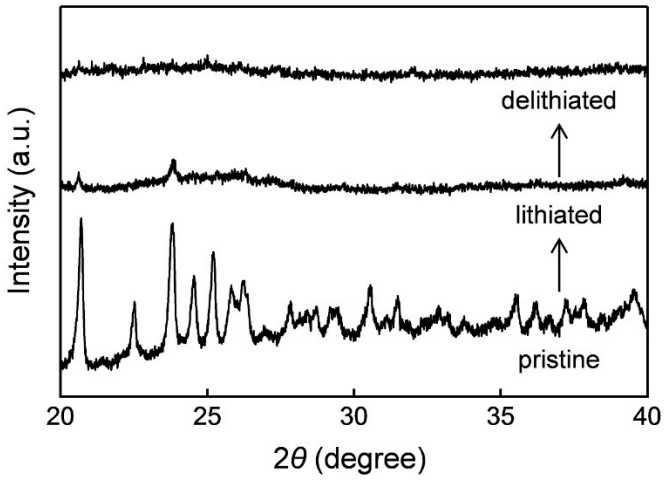

Figure S5. *Ex situ* X-ray diffraction patterns for $\{[Fe(Tp)(CN)_3]_2[Ni(H_2O)_2]\}\cdot 4H_2O$ upon (de)lithiation.

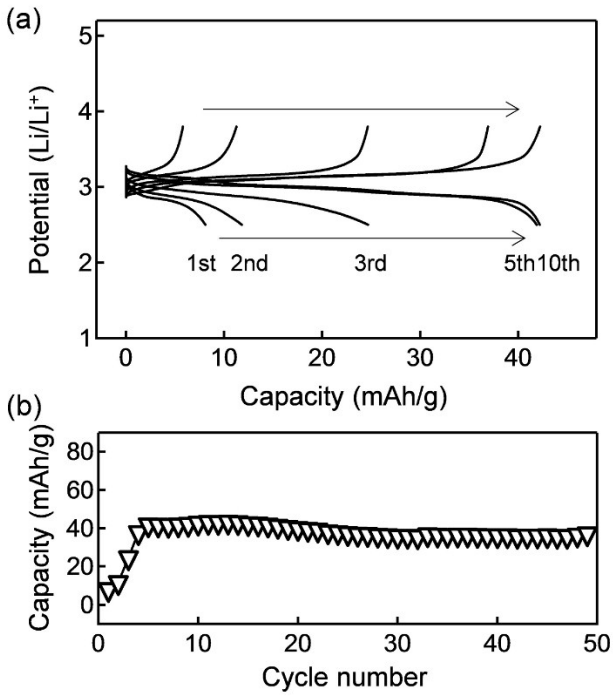

Figure S6. (a) Charge-discharge curves and (b) cycle stability of $\{[Fe(Tp)(CN)_3]_2[Ni(H_2O)_2]\}\cdot 4H_2O$ at the specific current of 10 mA/g.

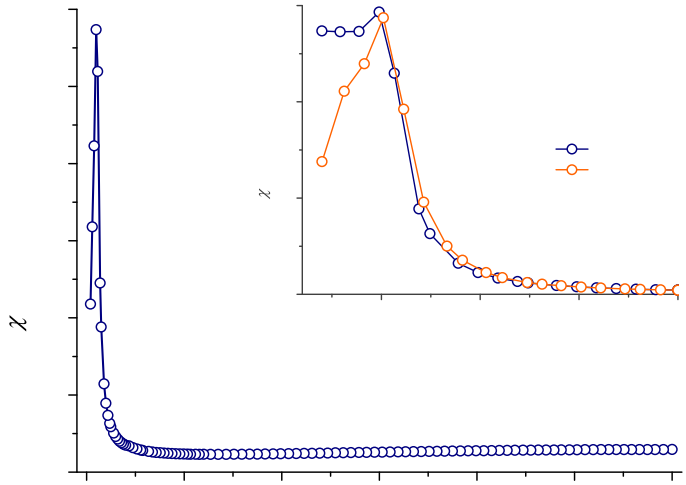

Figure S7. Thermal dependence of the $\chi_M T$ product of **1** in the temperature range 1.9-300 K under magnetic fields of 250 Oe (T < 20 K) and 2500 Oe (T > 20 K). The inset shows the zero-field-cooled and field-cooled magnetization curves (H = 250 Oe).

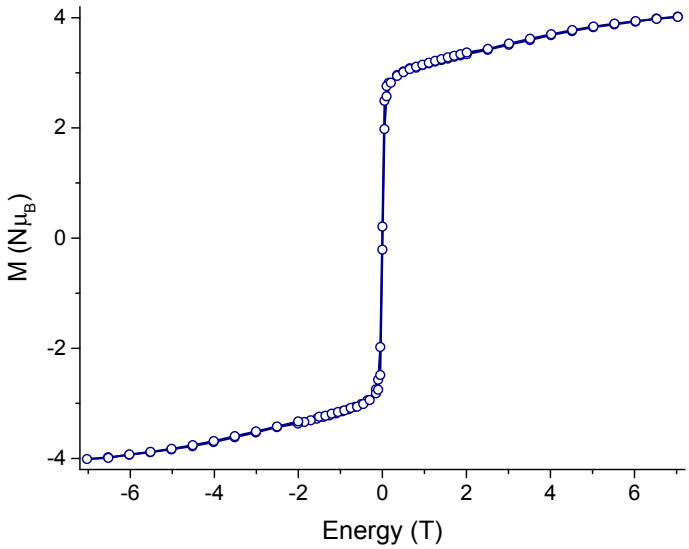

Figure S8. Plot of the magnetization *versus* magnetic field measured at 2.0 K: (o) experimental; (—) eye-guideline.

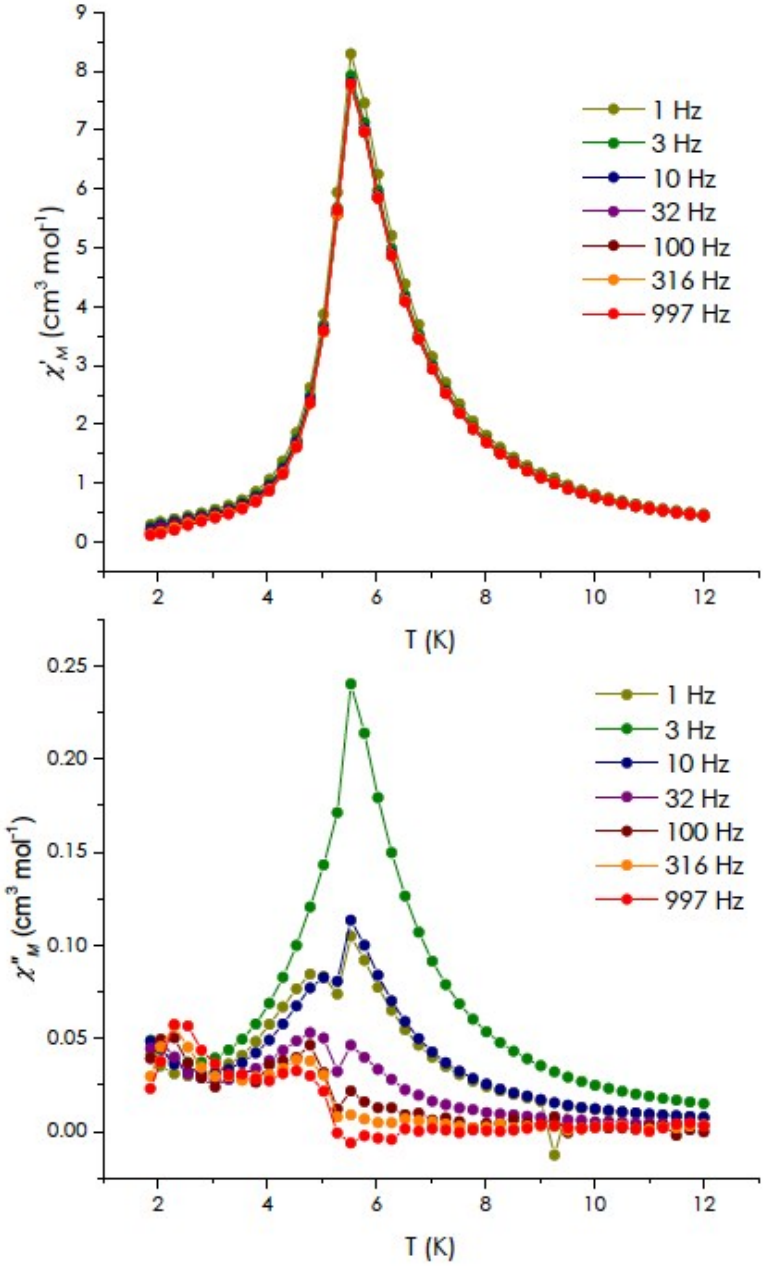

Figure S9. In-phase (top) and out-of-phase susceptibility measurements on **1** (H_{ac} = 3 Oe, H_{dc} = 0 Oe).

The temperature dependence of the $\chi_M T$ product for **1** [χ_M is the magnetic susceptibility per $Fe^{III}_2Ni^{II}$ unit] is shown in Fig. S5 above. The $\chi_M T$ value measured at 300 K, 2.9 cm^3 mol^{-1} K, is coherent with the expected value for the three isolated ions : one octahedral nickel(II) ion (S_{Ni} = 1) and two low-spin Fe^{III} centers (S=1/2) exhibiting a significant orbital contribution arising form the $^2T_{2g}$ ground term.[7] Upon cooling, the $\chi_M T$ value decreases smoothly and reaches a broad minimum near 65 K, with $\chi_M T$ = 2.3 cm^3 mol^{-1} K. Below this temperature, the $\chi_M T$ value

[7] R. Lescouëzec, J. Vaissermann, F. Lloret, M. Julve, M. Verdaguer , *Inorg. Chem.*, 2002, **41**, 23, 5943

strongly increases to reach a maxima of 57.4 cm^3 mol^{-1} K at 5 K, and finally it falls down to 21.8 cm^3mol^{-1} K at 1.9 K. The small decrease from room temperature to 65 K can be explained by the effect of the spin-orbit coupling in the anisotropic $[Fe^{III}(Tp)(CN)_3]^-$ complex. Below 50 K, the strong increase of the $\chi_M T$ value unambiguously points to the occurrence of a ferromagnetic interaction. Actually ferromagnetic interactions are usually observed in cyanide bridged Fe^{III}_{LS}-Ni^{II} complexes.[8] The ferromagnetic ground state is also confirmed by the magnetization versus field curve (Fig. S6), which increases very sharply at low field, and shows a value of 4.0 BM at 7 T (in agreement with a parallel alignment of the two S_{Fe} = ½ and the S_{Ni} = 1). The Field-Cooled and Zero-Field Cooled magnetization (FC-ZFC) curves (Fig. S5, inset) indicates the occurrence of a magnetic ordering at 5 K. This is confirmed by the ac magnetic measurement (Fig. S7), which show that the ac susceptibility exhibits a frequency independent maximum near 5 K. Overall, the magnetic properties of the dehydrated phase are very similar to that observed on fresh crystals of **1'** (reported by Wen *et al*.). The disappearance of the weak metamagnetism in **1** as compared to that observed on the fresh crystals of **1'** is likely associated to the change in the interchain magnetic interaction upon removal of the solvent molecules.

[8] see for example: (a) L. Toma, L. M. Toma, R. Lescouëzec, D. Armentano, G. De Munno, M. Andruh, J. Cano, F. Lloret, M. Julve, *Dalton Trans.* 2005, 1357 ; (b) L.M. Toma, R. Lescouëzec, S. Uriel, R. Llusar, C. Ruiz-Perez, J. Vaissermann, F. Lloret, M. Julve, *Dalton Trans*. 2007, 3690 ; (c) V. Costa, R. Lescouëzec, J. Vaissermann, P. Herson, Y. Journaux, M. H. Araujo, J. M. Clemente-Juan, F. Lloret, M. Julve, *Inorg. Chim. Acta*, 2008, 3912.

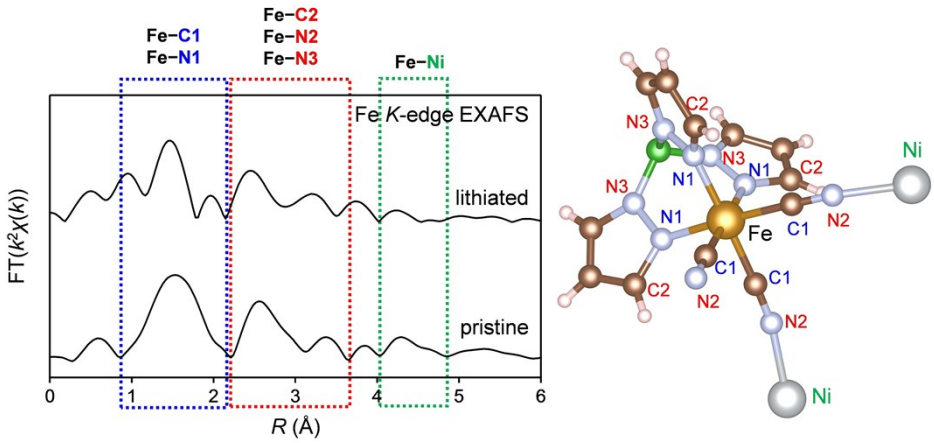

Figure S10. Fourier transform magnitudes weighted by k^2 of Fe *K*-edge EXAFS before and after Li^+ intercalation of **1**. The detailed analysis is difficult due to the existence of too many different atoms near the Fe atom. The bending of the cyanide link Fe-CN-Ni can also be affected by the Li intercalation and it can explain the broadening of some features if Fe coordination sites with different distortion coexist in the final amorphous intercalated samples. However this preliminary result shows that the coordination sphere of the Fe is not significantly altered.